

Textual and Visual Characteristics of Mathematical Expressions in Scholar Documents

Vidas Daudaravicius

UAB VTeX / Lithuania

vidas.daudaravicius@vtex.lt

Abstract

Mathematical expressions (ME) are widely used in scholar documents. In this paper we analyze characteristics of textual and visual MEs characteristics for the image-to- \LaTeX translation task. While there are open datasets of \LaTeX files with MEs included it is very complicated to extract these MEs from a document and to compile the list of MEs. Therefore we release a corpus of open-access scholar documents with PDF and JATS-XML parallel files. The MEs in these documents are \LaTeX encoded and are document independent. The data contains more than 1.2 million distinct annotated formulae and more than 80 million raw tokens of \LaTeX MEs in more than 8 thousand documents. While the variety of textual lengths and visual sizes of MEs are not well defined we found that the task of analyzing MEs in scholar documents can be reduced to the subtask of a particular text length, image width and height bounds, and display MEs can be processed as arrays of partial MEs.

1 Introduction

Mathematics is recognized as the most ancient scientific field in the world. Symbols were used from the beginning of mathematics. A specific breakthrough in mathematical language was the invention of the *equals* symbol ($=$) that is now universally accepted in mathematics, which was first recorded by the Welsh mathematician Robert Recorde in *The Whetstone of Witte* (1557)¹. Mathematics became the language of symbols to ease mathematical writing, reading and reasoning. Mathematical expressions (ME) are widely used phenomena in scholar documents but we know just little about the textual and visual characteristics of these MEs as this field is less studied in NLP do-

¹https://en.wikipedia.org/wiki/Equals_sign

main. The language of MEs is not linear as for instance the English language. Instead, every mathematical symbol has various types of relations, and these relations are vertically and visually represented in 2D space.

The majority of scholar documents is produced in PDF format. The main advantage of this format that it is a universal and human readable format on many devices. PDF also has many advancements for adopting the content of documents for machines by creating *tagged PDF*, though these features are used occasionally. In general, a PDF file contains layout specifications of fonts and their attributes, and no explicit labels are available for mathematics. Many researchers are struggling with the replication of MEs in other documents. Being able to automatically identify and decode mathematics (Lin et al., 2011; Wang and Liu, 2017a,b) in PDF files will enable a wide range of high-level applications such as information retrieval, machine reading, similarity analysis, information aggregation, and reasoning. Siegel et al. (2018) discuss how to recover the positional information of figures in PDF files. The proposed methods could be also used for the alignment of MEs in PDF and XML files. There are also efforts to automatically decode image MEs into \LaTeX (Deng et al., 2016, 2017). The length and size of MEs in scholar documents are little discussed. We find that researchers apply specific bounds to the textual length and visual size of MEs without any explanation. Therefore, our interest is to find out specific characteristics of MEs in scholar documents to be used for machine learning.

The *Mathematical REtrieval Collection* (MREC) (Líška et al., 2011) is a subset of the *arXMLiv* corpus and includes documents that were successfully converted to XML. MREC consists of well-formed XHTML documents.

MathML, a W3C standard, is used for representation of mathematical formulas. This corpus contains XHTML files only.

2 Markups and MEs

In general, all MEs in scholar documents can be read out loud as a linear sequence of words. The pseudo-linearity allows to embed MEs into natural language texts despite the visual multi-dimensional representation. This is a big advantage for humans to be able to combine natural language and symbolic language into one text. But it is not easy for machines to recognize the content and structure of these MEs.

There are several editors and markups for MEs. OpenOffice and MS Office® have internal support for writing MEs using special editors. These editors are frequently used when documents are not highly loaded with MEs, and they are sufficient for most users. The L^AT_EX typesetting system is used as the main technology in mathematics, physics, and other related domains. L^AT_EX is widely accepted because of its simplicity for humans to write and read MEs in linear order and to get very complex ME representations. *MathML*² is the only standardized markup for MEs which preserves content and layout. Both markups, L^AT_EX and MathML, are supported by the JATS NISO standard³. For instance, the representation of the formula

$$1 - e^{-\frac{1}{2}|x|^2} \quad (1)$$

in L^AT_EX is:

```
$1 - {\mathrm{e}}^{-\frac{1}{2}|x|^2}$
```

whereas in MathML it is:

```
<mml:math>
<mml:mn>1</mml:mn><mml:mo>-</mml:mo><mml:msup>
<mml:mrow><mml:mi mathvariant="normal">e</mml:mi>
</mml:mrow><mml:mrow><mml:mo>-</mml:mo>
<mml:mstyle displaystyle="false"><mml:mfrac>
<mml:mrow><mml:mn>1</mml:mn></mml:mrow>
<mml:mrow><mml:mn>2</mml:mn></mml:mrow>
</mml:mfrac></mml:mstyle><mml:mo stretchy="false">|
</mml:mo><mml:mi mathvariant="italic">x</mml:mi>
<mml:msup><mml:mrow><mml:mo stretchy="false">|
</mml:mo></mml:mrow><mml:mrow><mml:mn>2</mml:mn>
</mml:mrow></mml:msup></mml:mrow></mml:msup>
</mml:math>
```

Both representations are equal but the readability for humans and for computers are obviously discrepant. For humans, the L^AT_EX representation is easy to read, edit and interpret⁴. But L^AT_EX data

²Mathematical Markup Language (MathML) Version 3.0 2nd Edition

³JATS: Journal Article Tag Suite, version 1.2

⁴The first resource for mathematics **zbMATH** formula search uses the **MathWebSearch** system, which is a content-

has no explicit structural representation and advance knowledge is necessary to interpret ME entities and relations. On the other side, MathML data are well structured, relations and bounds of entities are explicitly defined in the data itself. Therefore, we often find both markup representations in scholar documents on-line.

3 Tokenization of L^AT_EX MEs

In this section we analyze the tokenization task of MEs encoded in L^AT_EX. Usually, tokenization is the first task of data preprocessing when a long sequence of information is split into words. Frequently, a white-space character is used to separate words. L^AT_EX allows to use white-space characters in MEs and these white-space characters usually do not affect the visual representation of MEs. For instance,

```
$1 - {\mathrm{e}}^{-\frac{1}{2}|x|^2}$
```

and

```
$ 1 - { \mathrm { e } } ^ { - \frac { 1 } { 2 } | x | } ^ { 2 } $
```

will result into the same ME image of Formula 1. Sometimes researchers need to insert some text into an ME or use a different approach for encoding variables. Often `\text` or `\mbox` are used for this purpose. The content of these commands is switched into L^AT_EX mode and, therefore, a white-space character becomes important and influences image rendering. Tokenization by inserting white-spaces

```
$ 1 - { \text { e } } ^ { - \frac { 1 } { 2 } | x | } ^ { \text { 2 } } $
```

will result to slightly different output:

$$1 - e^{-\frac{1}{2}|x|^2}.$$

White-space characters should not be used straightforwardly for the separation of tokens and should be used with caution. White-space characters should also be included into the vocabulary of ME tokens for the image-to-text task.

Tokenization of MEs is a task of splitting text into minimal meaningful LaTeX tokens, and tokenization should not affect image rendering. A sequence of letters in an ME often denotes a sequence of unique variables visually not split with white-space character. Variables often are single

based search engine for MathML formulas based on substituting tree indexing. A query should be inserted in L^AT_EX, but the database is MathML based.

letters and there is no evident sign for the boundaries of each variable. Single characters and numbers can be used as single tokens in most cases. We suggest to use a TAB or other specific character as a split character for tokenization.

4 The corpus of open-access scholar documents

We collected 8599 open-access scholar documents that are freely accessible on-line, that have both PDF and xhtml versions, include MEs at least once, and are under CC BY, CC BY NC, or CC BY NC SA licence⁵. The documents were published between 2012 and 2018. The majority of documents are research papers in the following journals:

- *Advances in Difference Equations* (2283 documents)
- *Boundary Value Problems* (1457 documents)
- *Fixed Point Theory and Applications* (1101 documents)
- *Journal of Inequalities and Applications* (2645 documents)

The average number of MEs per document is 291, and the average number of distinct MEs is 193⁶. In Figure 1 we can see that the number of distinct MEs is linearly increasing with the corpus size. This observation shows that the variety of MEs is very complex and new MEs are introduced in each document. This observation is very intriguing as we expected to see the very common distribution called 'heavy tail', Zipf, or other names of the same idea. We also observe that the typical MEs and distinct MEs ratio in each document is similar and equals to 1.5. This means that about 60 percent of MEs are duplicated in the document. The rest of the MEs are unique. The total number of MEs in the corpus is 2.5 million and the number of distinct MEs is 1.2 million. The maximum number of MEs in one document is 2671⁷. There are several documents that have only one ME.

In Figure 2 we observe the vocabulary size in the corpus of MEs. Vocabulary size does not increase significantly when a corpus is doubled from 40 million tokens to 80 million tokens. There are 39 types out of 728 types in total that occur only

⁵The compiled corpus of PDFs, JATS NISO XML files and list of mathematical expressions are available for download at <http://textmining.lt/OAScholarXML/>.

⁶Hereafter, we use JATS XML files to extract \LaTeX MEs.

⁷<http://dx.doi.org/10.1186/s13662-015-0541-4>

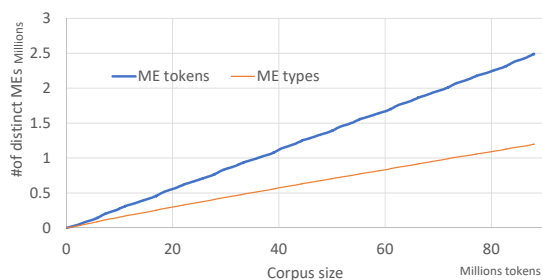


Figure 1: The increase of the number of \LaTeX MEs.

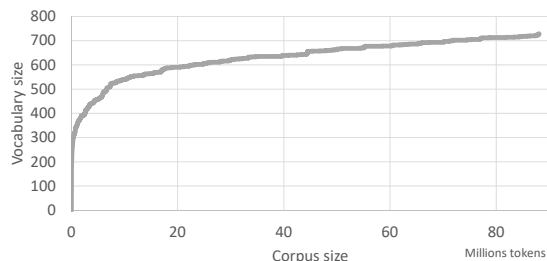


Figure 2: The increase of the vocabulary size of \LaTeX tokens.

once in the corpus. And there are 135 types that occur less than ten times in the corpus. The majority in vocabulary are \LaTeX commands. The most frequent tokens are `{`, `}`, `_` and `^`. The most frequent \LaTeX command is `\frac`. This shows that the vocabulary of MEs is small and already saturated. We could expect 1000 as vocabulary size upper limit of MEs for very large corpora.

5 Analysis of textual and visual characteristics

In this section we analyze the length of MEs encoded in \LaTeX . For the image-to- \LaTeX translation task Deng et al. (2017) uses a strict length range which falls in between 40 and 1024 characters and which is limited to 150 tokens. These bounds are used for training data and generated MEs. The paper does not describe the procedure of bounds settings. Do these bounds falsify the real world of MEs and do they consider only some part of the problem?

It is important to differentiate MEs (1) that are used as part of regular text and are placed on the same text line (*inline mode*), and (2) that are placed on a separate line and usually take more than one regular text line (*display mode*). The same ME in *inline* and *display* modes have slightly different visual layout and size. Therefore, we dif-

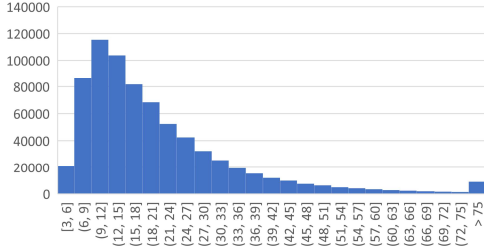


Figure 3: The \LaTeX length histogram of inline MEs.

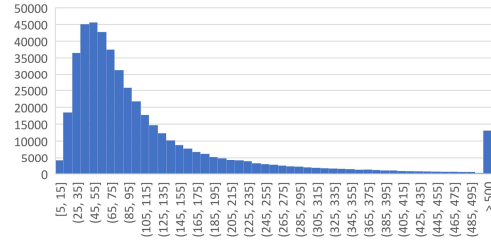


Figure 7: The \LaTeX length histogram of display MEs.

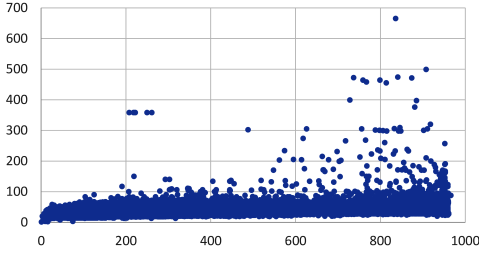


Figure 4: Width (x-axis) and height (y-axis) of rendered inline ME images in pixels (200 dpi).

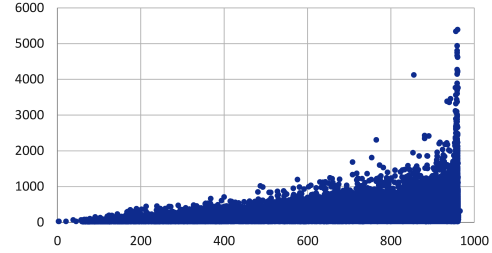


Figure 8: Width (x-axis) and height (y-axis) of rendered display ME images in pixels (200 dpi).

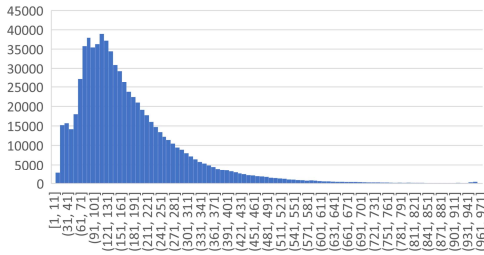


Figure 5: The image width histogram of inline MEs.

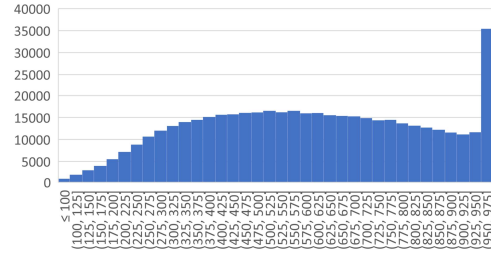


Figure 9: The image width histogram of display MEs.

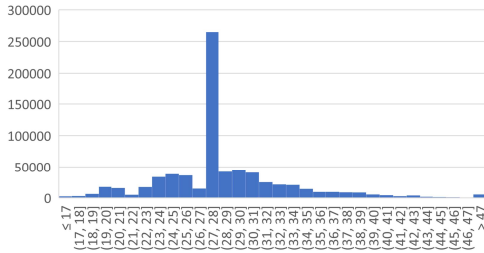


Figure 6: The image height histogram of inline MEs.

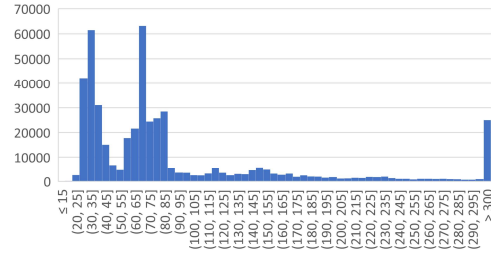


Figure 10: The image height histogram of display MEs.

ferentiate analysis of inline and display MEs.

5.1 Inline MEs

Inline MEs are often short insertions of symbolic language into regular text and they are not spread across many text lines. There are 732498 distinct inline MEs in the corpus. In Figure 3 we observe that the peak length in the list of distinct inline MEs is around 10 tokens and it slowly goes down until 75 tokens. In inline mode formulae that are longer than 75 tokens length we often find an

`\displaystyle` switch which turns inline formulae into display formulae. The longest inline ME is 1008 tokens (see Appendix B). Thus, the upper limit of complex inline formula is around 100 token. The most frequent inline ME is $\{x_n\}$, which occurs 13937 times, and is encoded as `\{x_{n}\}` that is 9 tokens length.

We rendered images of all MEs using the `shell` script in Appendix A. Rendered images have 200dpi resolution. In Figure 4 we show a variety of image sizes in pixels. The heights

of images fall into the range between 1 and 100 with some odd image height of over 100 pixels. The widths of images are in the range between 1 and 1000 pixels⁸. Figure 4 does not emphasize a specific inline image height and width except the ranges. In Figure 5 we observe the wide range distribution of rendered images. The majority of images are in the range between 30 and 500 pixels. In Figure 6 we observe a specific image height at which the majority of images were rendered. The majority of inline images have a height of 27 or 28 pixels. All other image heights of inline images are less frequent. Therefore, for the ME detection in PDF scholar documents we can expect a formula image size of 30-500 pixels width and 27-28 pixels height. Deng et al. (2017) uses groups of 128, 160, 192, 224, 256, 320, 384, 480 pixels image widths and 32, 64, 96, 128, 160 pixels image heights for the image-to- \LaTeX translation task. We can see that image size boxes are very similar to what we observe in our corpus.

5.2 Display MEs

Display MEs are insertions of symbolic language in text and occur in a document as a separate area from the regular text and can be spread over several text lines. There are 467056 distinct display MEs in our corpus. The most frequent display ME occurs 59 times in 55 documents and is 27 tokens length:

$$\lim_{n \rightarrow \infty} \|x_{n+1} - x_n\| = 0.$$

This low frequency shows the trend that display MEs are unique and we should not expect occurrence of the same formula in many places. This explains the linear growth of unique MEs in the corpus (see Figure 1). The longest display ME is 13987 tokens length (see Appendix C). Display MEs are very long and many of them can be over 500 tokens in length (see Figure 7). The majority of display formulae range from 20 to 250 tokens. It is definitely much longer than Deng et al. (2017) bound that is 150 tokens.

The display formula image size ranges from 5 to 1000 pixels width and 5 to 6000 pixels height. There is some dependency between the image width and height. If the image height is over 2000 pixels then the image width is always expected to be close to 1000 pixels. In Figure 9 we observe a wide range of frequent image widths and there are many of them at the maximum image width. So,

⁸1000 pixels take the full page width.

the image width mentioned in Deng et al. (2017) is too low for many display MEs. In Figure 10 we observe that the majority of display formulae height is at 30-35 and 65-70 pixels. The image height range between 30-35, which is close to inline formulae image height. This shows that many display formulae fit on a regular text line height. 65-70 pixels height is enough to visualize complex mathematical expressions such as \sum or \prod and it also fit on one line. Display formulae are very complex for the image-to- \LaTeX translation task as the text length is much longer than current Deep Neural Networks (DNN) can embed, and image height is too high to feed it to the DNN input. The solution to the problem could be to split display images into arrays of single line display images and to implement the image-to- \LaTeX task as a list of partial display images. For this we should also align break points in \LaTeX code and images. In general, this is not very complicated as there are clear clues in \LaTeX code (e.g., `\` or `\cr` commands) and in an image (e.g., horizontal gap between lines).

6 Conclusions

We release the corpus of more than 8000 open-access, JATS-NISO-XML tagged and PDF parallel scholar documents which contain at least one mathematical expression. Our analysis shows that inline MEs and display MEs have different textual and visual characteristics. Further, a display mathematical expression should be used as an array of partial mathematical expressions that each fit on one visual line. The textual length of inline MEs ranges between 5 to 75 tokens, image width ranges between 30 to 500 pixels, and image height ranges between 20 to 40 pixels. Display ME textual length ranges from 15 to more than 500 tokens, image width ranges between 100 to 1000 pixels, and image height ranges between 20 to more than 300 pixels. The partial display image height ranges between 20 to 85 pixels. These bounding settings include the majority of all mathematical expressions and can be used for image-to- \LaTeX translation task implementation.

Acknowledgments

This work was partially funded by Lithuanian Business Support Agency (Grant No J05-LVPA-K-03-0016).

References

- Yuntian Deng, Anssi Kanervisto, Jeffrey Ling, and Alexander M. Rush. 2017. [Image-to-markup generation with coarse-to-fine attention](#). In *Proceedings of the 34th International Conference on Machine Learning*, volume 70 of *Proceedings of Machine Learning Research*, pages 980–989, International Convention Centre, Sydney, Australia. PMLR.
- Yuntian Deng, Anssi Kanervisto, and Alexander M. Rush. 2016. What you get is what you see: A visual markup decompiler.
- Xiaoyan Lin, Liangcai Gao, Zhi Tang, Xiaofan Lin, and Xuan Hu. 2011. [Mathematical formula identification in pdf documents](#). pages 1419–1423.
- Martin Líška, Petr Sojka, Michal Růžička, and Petr Mravec. 2011. [Web Interface and Collection for Mathematical Retrieval: WebMiaS and MREC](#). In *Towards a Digital Mathematics Library.*, pages 77–84, Bertinoro, Italy. Masaryk University.
- Noah Siegel, Nicholas Lourie, Russell Power, and Waleed Ammar. 2018. [Extracting scientific figures with distantly supervised neural networks](#). *CoRR*, abs/1804.02445.
- Xing Wang and Jyh-Charn Liu. 2017a. [A content-constrained spatial \(ccs\) model for layout analysis of mathematical expressions](#). pages 334–339.
- Xing Wang and Jyh-Charn Liu. 2017b. [A font setting based bayesian model to extract mathematical expression in pdf files](#). pages 759–764.

A shell script for rendering png images with pdflatex

```
#!/bin/sh

cd "$1"
pdflatex -jobname "$2"
"\documentclass[border=2pt]{standalone}\usepackage{amsmath}\usepackage{amssymb}
\usepackage{upgreek}\usepackage{mathrsfs}\usepackage{wasysym}
\usepackage{esint}\usepackage{varwidth}\begin{document}
\begin{varwidth}{\linewidth}
\$\$
\end{varwidth}\end{document}"

convert -density 200 $2.pdf -quality 100 -colorspace RGB $2.png

convert $2.png -trim $2.png
rm $2.pdf $2.log $2.aux

texlive and imagemagic packages should be on your system to run a sample command:
$./formula path filename "$$\sqrt{\frac{1}{2}}$$"
```

B The longest inline mathematical expression ⁹

$$A_3 = p_1(a_1d_1^2\mu\hat{I}\hat{P} + a_1d_1q_1\mu\hat{I}\hat{P} + a_1d_1^2d_2\hat{I}^2\hat{P} + a_1d_1d_2q_1\hat{I}^2\hat{P} + a_1d_1^2q_2\hat{I}^2\hat{P} + a_1d_1q_1q_2\hat{I}^2\hat{P}) + (p_1 - \tau_1)(a_1d_1q_1\mu\hat{I}\hat{P}) + a_1q_1^2\mu\hat{I}\hat{P} + a_1d_1d_2q_1\hat{I}^2\hat{P} + a_1d_2q_1^2\hat{I}^2\hat{P} + a_1d_1q_1q_2\hat{I}^2\hat{P} + a_1q_1^2q_2\hat{I}^2\hat{P}) + p_2(-a_2d_2^2r\hat{I}\hat{M} - a_2d_2q_2r\hat{I}\hat{M} - a_2d_2^2\gamma\hat{I}\hat{M} - a_2d_2q_2\gamma\hat{I}\hat{M} + a_2d_1d_2^2\hat{I}^2\hat{M} + a_2d_2^2q_1\hat{I}^2\hat{M} + a_2d_1d_2q_2\hat{I}^2\hat{M} + a_2d_2q_1q_2\hat{I}^2\hat{M} + \frac{2a_2d_2^2r\hat{I}\hat{M}\hat{P}}{K} + \frac{2a_2d_2q_2r\hat{I}\hat{M}\hat{P}}{K} + (p_2 - \tau_2)(a_2d_2q_2r\hat{I}\hat{M} + a_2q_2^2r\hat{I}\hat{M} + a_2d_2q_2\gamma\hat{I}\hat{M} + a_2q_2^2\gamma\hat{I}\hat{M} - a_2d_1d_2q_2\hat{I}^2\hat{M} - a_2d_2q_1q_2\hat{I}^2\hat{M} - a_2d_1q_2^2\hat{I}^2\hat{M} - \frac{2a_2d_2q_2r\hat{I}\hat{M}\hat{P}}{K} - \frac{2a_2q_2^2r\hat{I}\hat{M}\hat{P}}{K})$$

C The longest display mathematical expression ¹⁰

$$\begin{aligned} \phi^{(1)} &= -\frac{1}{8}e^{\frac{i}{2}(-x-t\alpha+2t\alpha\beta)}\sqrt{2}(-2it^2\alpha^2 - 4t\alpha + 2t^2\alpha^2 + 2x^2 + 1 + i + 4xt\alpha \\ &\quad - 4ixt\alpha - 4ixt\alpha\beta^2 + 4it\alpha\beta^2 - 2t^2\alpha^2\beta^4 - 4x + 2i\alpha^2\beta^4t^2 \\ &\quad - 4it^2\alpha^2\beta^2 - 4xt\alpha\beta^2 - 4\alpha^2\beta^2t^2 - 2ix^2), \\ \psi^{(1)} &= \frac{i}{8}e^{-\frac{i}{2}(-x-t\alpha+2t\alpha\beta)}\sqrt{2}(2x^2 + 4x - 2it^2\alpha^2 + 1 + i \\ &\quad - 4ixt\alpha + 4t\alpha + 2t^2\alpha^2 - 4it\alpha\beta^2 - 4xt\alpha\beta^2 - 4\alpha^2\beta^2t^2 \\ &\quad - 4ixt\alpha\beta^2 + 2i\alpha^2\beta^4t^2 + 4xt\alpha - 4it^2\alpha^2\beta^2 - 2ix^2 - 2t^2\alpha^2\beta^4), \\ \phi^{(2)} &= -\frac{1}{192}e^{\frac{i}{2}(-x-t\alpha+2t\alpha\beta)}\sqrt{2}(-12 + 48t^2\alpha^2\beta^2 + 60x - 24xt\alpha + 8it^3\alpha^3\beta^6 + 8t^3\alpha^3 \\ &\quad + 36it\alpha\beta^2 - 24t^3\alpha^3\beta^2 + 8t^3\alpha^3\beta^6 + 24x^2t\alpha + 24xt^2\alpha^2 - 24t^3\alpha^3\beta^4 + 48b_1 \\ &\quad - 48ixt^3\alpha^3\beta^4 + 240ixt\alpha - 24xt^2\alpha^2\beta^4 - 24x^2t\alpha\beta^2 - 48xt^2\alpha^2\beta^2 + 12\alpha\beta^2t \\ &\quad + 60t\alpha - 12x^2 - 12t^2\alpha^2 + 48xt\alpha\beta^2 + 48t\alpha\beta^2b_1 - 48t\alpha\beta^2d_1 + 48x^2t^2\alpha^2\beta^2 \\ &\quad + 48xt^3\alpha^3\beta^2 - 16t^3\alpha^3\beta^6x + 16x^3t\alpha\beta^2 - 48b_1x - 48xd_1 - 48tab_1 - 48t\alpha d_1 \\ &\quad + 12t^2\alpha^2\beta^4 + 16t^4\alpha^4\beta^2 - 16t^4\alpha^4\beta^6 + 120ix^2 - 24ix^2t^2\alpha^2\beta^4 + 48it\alpha\beta^2d_1 \\ &\quad - 48ixt^2\alpha^2\beta^2 - 24ix^2t\alpha\beta^2 - 24it^4\alpha^4\beta^4 + 24it^2\alpha^2\beta^2 - 24ixt^2\alpha^2 + 8x^3 \\ &\quad - 24ix^2t\alpha + 48id_1 + 48it\alpha\beta^2b_1 + 4ix^4 + 24ix^2t^2\alpha^2 + 48itab_1 + 24ixt\alpha\beta^2 \\ &\quad + 24ixt^2\alpha^2\beta^4 + 24it^3\alpha^3\beta^4 - 8ix^3 + 15i - 84ix + 72it^2\alpha^2\beta^4 - 48it\alpha d_1 \\ &\quad - 24it^3\alpha^3\beta^2 + 16ix^3t\alpha + 4it^4\alpha^4\beta^8 + 120it^2\alpha^2 + 48ib_1x + 4it^4\alpha^4 \end{aligned}$$

⁹See the original formula at Chaudhary, M., Pathak, R. *A dynamical approach to the legal and illegal logging of forestry population and conservation using taxation* *Advances in Difference Equations* (2017) 2017:385.

¹⁰See the original formula at Wen *Advances in Difference Equations* (2016) 2016:311. This kind of formula is automatically generated by the specific algorithms to mathematically describe some phenomenon.

$$\begin{aligned}
& -84it\alpha - 8it^3\alpha^3 - 48ixd_1 + 16it^3\alpha^3x), \\
\psi^{(2)} = & \frac{i}{192}e^{-\frac{i}{2}(-x-t\alpha+2t\alpha\beta)}\sqrt{2}(-12 + 48t^2\alpha^2\beta^2 - 60x - 24xt\alpha - 8t^3\alpha^3 + 24t^3\alpha^3\beta^2 \\
& - 8t^3\alpha^3\beta^6 - 24x^2t\alpha - 24xt^2\alpha^2 + 24t^3\alpha^3\beta^4 - 48b_1 - 36it\alpha\beta^2 + 16it^3\alpha^3x \\
& + 24xt^2\alpha^2\beta^4 + 24x^2t\alpha\beta^2 + 48xt^2\alpha^2\beta^2 - 12\alpha\beta^2t - 60t\alpha - 12x^2 - 12t^2\alpha^2 \\
& + 48xt\alpha\beta^2 + 48t\alpha\beta^2b_1 - 48t\alpha\beta^2d_1 + 48x^2t^2\alpha^2\beta^2 + 48xt^3\alpha^3\beta^2 - 16t^3\alpha^3\beta^6x \\
& + 16x^3t\alpha\beta^2 - 48b_1x - 48xd_1 - 48tab_1 - 48tad_1 + 12t^2\alpha^2\beta^4 + 16t^4\alpha^4\beta^2 \\
& - 16t^4\alpha^4\beta^6 - 24ixt^2\alpha^2\beta^4 + 24ix^2t\alpha + 48it\alpha\beta^2b_1 - 48itad_1 + 48itab_1 \\
& + 24it^3\alpha^3\beta^2 - 24ix^2t^2\alpha^2\beta^4 + 120it^2\alpha^2 + 48ib_1x - 24it^3\alpha^3\beta^4 + 240ixt\alpha \\
& + 48ixt^2\alpha^2\beta^2 + 72it^2\alpha^2\beta^4 + 120ix^2 - 48ixt^3\alpha^3\beta^4 + 24it^2\alpha^2\beta^2 + 16ix^3t\alpha \\
& + 8ix^3 - 8x^3 - 8it^3\alpha^3\beta^6 + 48it\alpha\beta^2d_1 + 84ix - 48id_1 + 24ixt^2\alpha^2 \\
& + 15i + 24ix^2t\alpha\beta^2 + 4it^4\alpha^4\beta^8 + 84it\alpha - 24it^4\alpha^4\beta^4 + 24ix^2t^2\alpha^2 + 4ix^4 \\
& + 4it^4\alpha^4 - 48ixd_1 + 8it^3\alpha^3 + 24ixt\alpha\beta^2), \\
\phi^{(3)} = & -\frac{1}{23,040}e^{\frac{i}{2}(-x-t\alpha+2t\alpha\beta)}\sqrt{2}(-405 - 1,440x^2d_1 - 1,440b_1x^2 - 5,760ixd_2 \\
& + 8t^6\alpha^6\beta^12 - 48t^6\alpha^6\beta^2 + 48it^5\alpha^5 - 8,100t^2\alpha^2\beta^2 - 6,840x^2t^2\alpha^2 + 2,880x \\
& - 120t^6\alpha^6\beta^8 - 1,440ib_1^2 + 1,440id_1^2 + 3,840ix^3 - 8ix^6 - 17,010ix^2 - 1,260ix^4 \\
& + 5,760id_2 + 48ix^5 - 1,440it\alpha\beta^2b_1 - 5,760tab_2 - 4,560xt^3\alpha^3 + 5,760ib_2x \\
& - 120t^4\alpha^4x^2 + 1,080t^4\alpha^4\beta^4 + 48it^5\alpha^5\beta^10x - 2,880ixt^2\alpha^2b_1 - 25,380xt\alpha \\
& - 17,010it^2\alpha^2 - 1,440ix^2d_1 + 240t^3\alpha^3 - 2,880ixd_1t\alpha + 1,440it^2\alpha^2\beta^4d_1 \\
& + 2,880it^3\alpha^3\beta^4b_1 - 2,880it^3\alpha^3d_1\beta^2 + 2,880it^2\alpha^2\beta^4b_1x - 2,880ix^2tab_1 \\
& - 2,880ix^2t\alpha\beta^2d_1 - 5,760ixd_1t^2\alpha^2\beta^2 - 720ix^2t\alpha\beta^2 - 1,440ixt^2\alpha^2\beta^2 \\
& + 2,880id_1b_1 - 480it^4\alpha^4\beta^6x^2 + 480ix^2t^4\alpha^4\beta^2 + 240it^5\alpha^5\beta^2x + 240ix^4t^2\alpha^2\beta^2 \\
& + 1,200it^3\alpha^3\beta^6x - 120it^4\alpha^4\beta^8x^2 + 480ixt^5\alpha^5\beta^4 + 720ix^2t^4\alpha^4\beta^4 \\
& + 480ix^3t^3\alpha^3\beta^4 + 48ix^5t\alpha\beta^2 + 5,220ixt\alpha\beta^2 + 7,920ixt^3\alpha^3\beta^2 + 7,920ix^2t^2\alpha^2\beta^2 \\
& + 2,640ix^3t\alpha\beta^2 + 120ix^4t^2\alpha^2\beta^4 - 240it^5\alpha^5\beta^8x - 480ix^3t^2\alpha^2\beta^4 \\
& + 240it^4\alpha^4\beta^8x - 14,400ib_1x - 1,440ixt^4\alpha^4\beta^4 - 1,440ix^2t^3\alpha^3\beta^4 - 4,560x^3t\alpha \\
& + 2,880ib_1xt\alpha\beta^2 + 2,880it^2\alpha^2b_1\beta^2 + 5,760t^3\alpha^3\beta^2 + 1,920t^3\alpha^3\beta^6 + 720x^2t\alpha \\
& + 720xt^2\alpha^2 - 720t^3\alpha^3\beta^4 + 13,140ix - 3,600b_1 - 5,040d_1 + 5,760b_2 \\
& - 5,760tad_2 - 960ix^3b_1 - 160it^3\alpha^3\beta^6x^3 - 8it^6\alpha^6 + 1,800ix^2t^2\alpha^2\beta^4 \\
& + 1,440ib_1x^2 + 3,840it^3\alpha^3 - 720xt^2\alpha^2\beta^4 + 5,760x^2t\alpha\beta^2 + 11,520xt^2\alpha^2\beta^2 \\
& + 1,620\alpha\beta^2t + 1,440ixd_1 + 2,880t\alpha - 1,260it^4\alpha^4 - 12,690x^2 - 12,690t^2\alpha^2 \\
& - 120x^4t^2\alpha^2 + 11,520ix^2t\alpha - 8,100xt\alpha\beta^2 - 2,880t\alpha\beta^2b_1 + 1,440t\alpha\beta^2d_1 \\
& - 9,360x^2t^2\alpha^2\beta^2 - 9,360xt^3\alpha^3\beta^2 + 2,160t^3\alpha^3\beta^4x - 720t^3\alpha^3\beta^6x - 3,120x^3t\alpha\beta^2 \\
& + 1,080x^2t^2\alpha^2\beta^4 - 1,140t^4\alpha^4 + 1,440b_1x + 14,400xd_1 - 1,140x^4 + 780t^4\alpha^4\beta^8 \\
& + 1,440tab_1 + 14,400tad_1 + 4,050t^2\alpha^2\beta^4 - 3,120t^4\alpha^4\beta^2 - 720t^4\alpha^4\beta^6 \\
& + 240it^3\alpha^3\beta^6 - 720it^3\alpha^3\beta^2 + 240ix^4t\alpha + 13,140it\alpha + 11,520ixt^2\alpha^2 \\
& - 2,880xt\alpha\beta^2d_1 - 1,440it^2\alpha^2d_1 + 480ix^3t^2\alpha^2 + 480it^3\alpha^3x^2 + 240it^5\alpha^5\beta^8 \\
& - 5,040it^3\alpha^3x - 34,020ixt\alpha - 5,040ix^3t\alpha + 2,610it^2\alpha^2\beta^4 + 1,440itad_1 \\
& + 660it^4\alpha^4\beta^8 - 7,560ix^2t^2\alpha^2 - 1,440t^2\alpha^2b_1 + 240t^5\alpha^5\beta^2 - 480t^5\alpha^5\beta^6
\end{aligned}$$

$$\begin{aligned}
& + 48t^5\alpha^5\beta^{10} - 1,440t^2\alpha^2d_1 + 960x^3d_1 - 5,760b_2x - 5,760xd_2 + 2,880d_1b_1 \\
& + 1,440b_1^2 - 8x^6 - 1,440d_1^2 + 5,760t\alpha\beta^2b_2 - 5,760t\alpha\beta^2d_2 + 2,880x^2t\alpha d_1 \\
& + 2,880xt^2\alpha^2d_1 - 2,880t^3\alpha^3\beta^4d_1 - 2,880t^3\alpha^3\beta^2b_1 + 960t^3\alpha^3\beta^6b_1 - 48x^5t\alpha\beta^2 \\
& + 160t^6\alpha^6\beta^6 - 160t^3\alpha^3x^3 - 48t^5\alpha^5x - 48t^6\alpha^6\beta^{10} + 960t^3\alpha^3d_1 - 48x^5t\alpha \\
& + 120t^6\alpha^6\beta^4 - 2,880x^2t\alpha\beta^2b_1 - 5,760xt^2\alpha^2\beta^2b_1 - 2,880xt^2\alpha^2\beta^4d_1 - 8t^6\alpha^6 \\
& - 240t^5\alpha^5\beta^2x + 480t^5\alpha^5\beta^6x - 240x^4t^2\alpha^2\beta^2 - 480x^3t^3\alpha^3\beta^2 + 480x^3t^3\alpha^3\beta^4 \\
& - 480x^2t^4\alpha^4\beta^2 + 720x^2t^4\alpha^4\beta^4 + 480xt^5\alpha^5\beta^4 + 160t^3\alpha^3\beta^6x^3 + 480t^4\alpha^4\beta^6x^2 \\
& - 120t^4\alpha^4\beta^8x^2 - 240t^5\alpha^5\beta^8x + 120x^4t^2\alpha^2\beta^4 - 48t^5\alpha^5\beta^{10}x - 14,400it\alpha b_1 \\
& - 960it^3\alpha^3b_1 + 3,600ixt^3\alpha^3\beta^4 + 480ix^3t^3\alpha^3\beta^2 + 5,220it^2\alpha^2\beta^2 - 48ix^5t\alpha \\
& + 5,760it\alpha b_2 - 160it^3\alpha^3x^3 - 120it^4\alpha^4x^2 - 120ix^4t^2\alpha^2 - 48it^5\alpha^5x - 120it^6\alpha^6\beta^8 \\
& + 120it^6\alpha^6\beta^4 + 240x^4t\alpha\beta^2 - 2,880xt\alpha b_1 - 2,880t^2\alpha^2\beta^2d_1 + 8it^6\alpha^6\beta^{12} \\
& + 1,200it^4\alpha^4\beta^6 + 2,640it^4\alpha^4\beta^2 - 160it^6\alpha^6\beta^6 + 48it^6\alpha^6\beta^2 - 480it^5\alpha^5\beta^4 \\
& + 240it^4\alpha^4x + 1,800it^4\alpha^4\beta^4 - 5,760it\alpha d_2 + 48it^6\alpha^6\beta^{10} + 1,440it^2\alpha^2b_1 \\
& + 240x^3 + 2,880it^2\alpha^2\beta^2d_1 + 2,880ixt\alpha\beta^2d_1 - 1,440it^2\alpha^2\beta^4b_1 + 1,440t^2\alpha^2\beta^4b_1 \\
& - 2,880xt\alpha d_1 + 2,880t^2\alpha^2\beta^2b_1 + 1,440t^2\alpha^2\beta^4d_1 + 960x^3t^2\alpha^2\beta^2 \\
& + 1,440x^2t^3\alpha^3\beta^2 + 960xt^4\alpha^4\beta^2 - 480t^3\alpha^3\beta^6x^2 - 960t^4\alpha^4\beta^6x - 3,600id_1 \\
& - 2,880it\alpha\beta^2d_1 + 5,760it\alpha\beta^2b_2 + 2,880ib_1xt\alpha - 1,395i + 5,040ib_1 \\
& + 2,880xt\alpha\beta^2b_1 + 960it^3\alpha^3\beta^6d_1 - 480it^5\alpha^5\beta^6x + 5,760it\alpha\beta^2d_2), \\
\psi^{(3)} = & \frac{i}{23,040} e^{-\frac{i}{2}(-x-t\alpha+2t\alpha\beta)} \sqrt{2} (-405 + 720it^3\alpha^3\beta^2 + 1,440x^2d_1 + 1,440b_1x^2 \\
& + 8t^6\alpha^6\beta^{12} - 48t^6\alpha^6\beta^2 - 8,100t^2\alpha^2\beta^2 - 6,840x^2t^2\alpha^2 - 2,880x \\
& + 480ix^3t^2\alpha^2\beta^4 - 120t^6\alpha^6\beta^8 - 1,440ib_1^2 - 5,760ixd_1t^2\alpha^2\beta^2 - 5,760ixd_2 \\
& - 5,760t\alpha b_2 - 4,560xt^3\alpha^3 + 2,880id_1b_1 - 2,880ixt^2\alpha^2b_1 - 120t^4\alpha^4x^2 \\
& + 1,080t^4\alpha^4\beta^4 - 25,380xt\alpha + 7,920ixt^3\alpha^3\beta^2 + 48it^5\alpha^5\beta^{10}x - 17,010it^2\alpha^2 \\
& - 240t^3\alpha^3 - 2,880ixt\alpha\beta^2d_1 - 1,260ix^4 - 4,560x^3t\alpha - 5,760t^3\alpha^3\beta^2 \\
& - 1,920t^3\alpha^3\beta^6 - 720x^2t\alpha - 720xt^2\alpha^2 + 720t^3\alpha^3\beta^4 + 5,760it\alpha b_2 + 3,600b_1 \\
& + 5,040d_1 - 5,760b_2 - 5,760t\alpha d_2 + 5,760ib_2x + 1,800ix^2t^2\alpha^2\beta^4 - 5,040ix^3t\alpha \\
& - 240it^5\alpha^5\beta^8 - 160it^3\alpha^3\beta^6x^3 - 2,880it\alpha\beta^2d_1 - 5,040it^3\alpha^3x - 1,440it\alpha\beta^2b_1 \\
& + 720xt^2\alpha^2\beta^4 - 5,760x^2t\alpha\beta^2 - 11,520xt^2\alpha^2\beta^2 - 1,620\alpha\beta^2t - 2,880t\alpha - 8it^6\alpha^6 \\
& - 12,690x^2 - 12,690t^2\alpha^2 - 120x^4t^2\alpha^2 + 120ix^4t^2\alpha^2\beta^4 + 240it^5\alpha^5\beta^2x \\
& - 8,100xt\alpha\beta^2 - 2,880t\alpha\beta^2b_1 + 1,440t\alpha\beta^2d_1 - 9,360x^2t^2\alpha^2\beta^2 - 9,360xt^3\alpha^3\beta^2 \\
& + 2,160t^3\alpha^3\beta^4x - 720t^3\alpha^3\beta^6x - 3,120x^3t\alpha\beta^2 + 1,080x^2t^2\alpha^2\beta^4 - 1,140t^4\alpha^4 \\
& + 1,440b_1x + 14,400xd_1 - 1,140x^4 + 780t^4\alpha^4\beta^8 + 1,440t\alpha b_1 + 14,400t\alpha d_1 \\
& + 4,050t^2\alpha^2\beta^4 - 3,120t^4\alpha^4\beta^2 - 720t^4\alpha^4\beta^6 + 2,880xt\alpha\beta^2d_1 - 480it^5\alpha^5\beta^6x \\
& - 160it^3\alpha^3x^3 + 1,440ixt^2\alpha^2\beta^2 - 1,440ib_1x^2 - 48it^5\alpha^5 + 1,440t^2\alpha^2b_1 \\
& - 240t^5\alpha^5\beta^2 + 480t^5\alpha^5\beta^6 - 48t^5\alpha^5\beta^{10} + 1,440t^2\alpha^2d_1 + 960x^3d_1 - 5,760b_2x \\
& - 5,760xd_2 + 2,880d_1b_1 + 1,440b_1^2 - 8x^6 - 1,440d_1^2 + 5,760t\alpha\beta^2b_2 \\
& - 5,760t\alpha\beta^2d_2 + 2,880x^2t\alpha d_1 + 2,880xt^2\alpha^2d_1 - 2,880t^3\alpha^3\beta^4d_1 \\
& - 2,880t^3\alpha^3\beta^2b_1 + 960t^3\alpha^3\beta^6b_1 - 48x^5t\alpha\beta^2 + 160t^6\alpha^6\beta^6 - 160t^3\alpha^3x^3 \\
& - 48t^5\alpha^5x - 48t^6\alpha^6\beta^{10} + 960t^3\alpha^3d_1 - 48x^5t\alpha + 120t^6\alpha^6\beta^4 - 2,880x^2t\alpha\beta^2b_1
\end{aligned}$$

$$\begin{aligned}
& - 5,760xt^2\alpha^2\beta^2b_1 - 2,880xt^2\alpha^2\beta^4d_1 - 8t^6\alpha^6 - 240t^5\alpha^5\beta^2x + 480t^5\alpha^5\beta^6x \\
& - 1,260it^4\alpha^4 - 240x^4t^2\alpha^2\beta^2 - 480x^3t^3\alpha^3\beta^2 + 480x^3t^3\alpha^3\beta^4 - 480x^2t^4\alpha^4\beta^2 \\
& + 720x^2t^4\alpha^4\beta^4 + 480xt^5\alpha^5\beta^4 + 160t^3\alpha^3\beta^6x^3 + 480t^4\alpha^4\beta^6x^2 - 120t^4\alpha^4\beta^8x^2 \\
& - 240t^5\alpha^5\beta^8x + 120x^4t^2\alpha^2\beta^4 - 48t^5\alpha^5\beta^10x + 48ix^5t\alpha\beta^2 + 2,640ix^3t\alpha\beta^2 \\
& + 48it^6\alpha^6\beta^10 + 480it^5\alpha^5\beta^4 - 2,880it^3\alpha^3d_1\beta^2 + 1,440ixt^4\alpha^4\beta^4 - 48ix^5 \\
& - 120it^6\alpha^6\beta^8 - 240x^4t\alpha\beta^2 + 2,880xt\alpha b_1 + 2,880t^2\alpha^2\beta^2d_1 - 120it^4\alpha^4\beta^8x^2 \\
& - 480it^4\alpha^4\beta^6x^2 + 7,920ix^2t^2\alpha^2\beta^2 - 960it^3\alpha^3b_1 + 2,880it^2\alpha^2\beta^4b_1x - 8ix^6 \\
& - 7,560ix^2t^2\alpha^2 + 2,640it^4\alpha^4\beta^2 - 240x^3 - 48ix^5t\alpha + 960it^3\alpha^3\beta^6d_1 \\
& + 48it^6\alpha^6\beta^2 + 1,440it\alpha d_1 - 14,400ib_1x - 14,400it\alpha b_1 + 5,760it\alpha\beta^2d_2 \\
& + 5,220ixt\alpha\beta^2 - 2,880ib_1xt\alpha\beta^2 + 1,440ix^2t^3\alpha^3\beta^4 - 1,440t^2\alpha^2\beta^4b_1 \\
& + 2,880xt\alpha d_1 - 2,880t^2\alpha^2\beta^2b_1 - 1,440t^2\alpha^2\beta^4d_1 - 960x^3t^2\alpha^2\beta^2 \\
& - 1,440x^2t^3\alpha^3\beta^2 - 960xt^4\alpha^4\beta^2 + 480t^3\alpha^3\beta^6x^2 + 960t^4\alpha^4\beta^6x + 480ixt^5\alpha^5\beta^4 \\
& - 120it^4\alpha^4x^2 - 13,140it\alpha + 3,600ixt^3\alpha^3\beta^4 - 2,880ix^2t\alpha b_1 + 8it^6\alpha^6\beta^{12} \\
& - 5,040ib_1 - 2,880ix^2t\alpha\beta^2d_1 - 160it^6\alpha^6\beta^6 - 5,760it\alpha d_2 - 240it^3\alpha^3\beta^6 \\
& - 13,140ix + 1,200it^3\alpha^3\beta^6x - 480ix^3t^2\alpha^2 + 1,440ixd_1 + 1,200it^4\alpha^4\beta^6 \\
& - 34,020ixt\alpha - 2,880it^2\alpha^2\beta^2d_1 - 1,440it^2\alpha^2\beta^4d_1 + 5,760it\alpha\beta^2b_2 \\
& - 2,880xt\alpha\beta^2b_1 + 480ix^3t^3\alpha^3\beta^4 + 720ix^2t\alpha\beta^2 - 48it^5\alpha^5x - 11,520ixt^2\alpha^2 \\
& + 240ix^4t^2\alpha^2\beta^2 - 2,880ib_1xt\alpha - 3,840it^3\alpha^3 - 3,840ix^3 + 1,440it^2\alpha^2d_1 \\
& - 5,760id_2 + 120it^6\alpha^6\beta^4 + 2,880ixd_1t\alpha + 480ix^3t^3\alpha^3\beta^2 - 2,880it^2\alpha^2b_1\beta^2 \\
& - 120ix^4t^2\alpha^2 + 660it^4\alpha^4\beta^8 - 480it^3\alpha^3x^2 + 1,440ix^2d_1 + 2,880it^3\alpha^3\beta^4b_1 \\
& + 1,440it^2\alpha^2\beta^4b_1 + 480ix^2t^4\alpha^4\beta^2 - 1,440it^2\alpha^2b_1 - 240it^5\alpha^5\beta^8x - 240it^4\alpha^4x \\
& + 720ix^2t^4\alpha^4\beta^4 + 1,800it^4\alpha^4\beta^4 - 17,010ix^2 - 1,395i + 1,440id_1^2 + 3,600id_1 \\
& - 11,520ix^2t\alpha - 960ix^3b_1 + 2,610it^2\alpha^2\beta^4 - 240it^4\alpha^4\beta^8x \\
& - 240ix^4t\alpha + 5,220it^2\alpha^2\beta^2).
\end{aligned}$$